

Dependence Structure Between Crypto-Asset ETFs and Other Financial Assets

Guilherme da Silva Correia^{†, a} 

Leandro de Almeida Rocco^{‡, a} 

^aUniversidade Federal do Ceará

Abstract Understanding the dynamics of dependency among financial assets is crucial for decision-making in the process of financial asset allocation. This study aims to estimate the dependency structure between ETFs based on crypto-assets (HASH11, QBTC11, and QETH11) and other traditional investment assets (BOVA11, GOLD11, IVVB11, EURP11, TIP, and SHY). It seeks to understand, through three vine copula models, whether exposure to the cryptocurrency market provides a hedging structure against conventional assets. The results indicate that these assets are strongly related to each other, moderately associated with the American and European markets, and weakly correlated with Brazil, gold, and U.S. bonds. Furthermore, they can serve as a hedge for the European and American markets and as a diversification option for the Chinese and Brazilian markets, gold, and short-term U.S. and inflation-indexed bonds.

Keywords: Dependence structure; ETF; Cryptoassets; Vine Copulas.

JEL codes: C32; C51; C52; C58; G15.

1. Introduction

Since the introduction of Bitcoin, through the white paper published by Nakamoto (2008), the cryptocurrency universe has expanded significantly with the emergence of thousands of new digital currencies. This proliferation has had a notable impact on global financial markets. These assets have become highly attractive due to the significant returns reported in recent years, and their nature has fostered the creation of a new investment ecosystem, which has become part of the portfolios of various financial market participants.

This asset class has delivered high returns over the past decade, being used as a hedging strategy against the volatility of conventional assets, fiat currencies, or geopolitical risks, and also as a portfolio diversification instrument. As Almeida and Gonçalves (2022) points out, there is evidence in the literature

How to cite: Correia, G. S. & Rocco, L. A. (2026). Dependence Structure Between Crypto-Asset ETFs and Other Financial Assets. *XXVI Encontro Brasileiro de Finanças*, Fortaleza.

[†] guilherme.scorreia18@gmail.com

[‡] lrocco@ufc.br

that these assets can be a good option for protecting portfolios against market risks; however, these properties vary over time and under external conditions.

Investing directly in these assets is not always straightforward, as it requires understanding how the digital wallets that store these digital currencies operate. Investors must ensure that their wallets are securely protected, since if access is lost due to forgetting the password or the private key, the investor completely loses access to their cryptocurrencies (Suratkar et al., 2020).

Given the anonymous, decentralized, globally accessible nature of these assets, their intermittent operation, and the lack of specific regulation in many countries, the cryptocurrency market has become fertile ground for various cybercrimes. Many crypto exchanges that distribute this asset class suffer constant attacks from hackers seeking to steal digital coins; there is a lack of transparency regarding the custody of users' funds on these platforms; and numerous cybercriminals create fake applications and cryptocurrencies to carry out financial scams (Xia et al., 2020).

Given these challenges, a new way to gain exposure to the digital currency market is through Exchange-Traded Funds (ETFs). Because they fall under the stock exchange structure, investing in an ETF entails some differences compared to investing directly in a cryptocurrency, making it a safer option in light of the regulatory framework that the financial institutions involved must follow. Moreover, the investment process is simplified—there is no need to deal with *exchanges*, which can quote significantly different prices for the same asset (Makarov and Schoar, 2020) and more secure, as it reduces concerns over the custody of the crypto-asset.

Another difference is that ETFs are traded on business days during stock-exchange operating hours, whereas in the cryptocurrency market, trading is possible at any time, allowing for rapid and unpredictable price movements outside of conventional hours.

In February 2021, the first crypto-asset ETF was launched in Canada and, a few months later, on the Brazilian stock exchange. The asset manager QR Asset Management conducted the initial public offering of QBTC11, whose benchmark index is the CME CF Bitcoin Reference Rate (Goeking, 2021). Since then, other managers have launched new ETFs related to the crypto ecosystem worldwide. Despite their recent emergence, by 2022 some of these cryptocurrency ETFs were already among the ten largest in Brazil by number of unitholders (Economatica, 2023), demonstrating the interest of many investors in adding this type of asset to their portfolios for diversification and returns.

This study aims to analyze the dependency structure between ETFs focused

on crypto-assets and those tied to traditional investment assets—such as equity indices, short-term U.S. Treasury bonds, and inflation-indexed securities. Although the literature includes works examining how cryptocurrencies relate to conventional assets (Charfeddine and Benlagha, 2016; Jeribi and Fakhfekh, 2021; Osman et al., 2023), the distinguishing feature of this paper lies in its focus on a new class of ETFs that offer an alternative and simplified way to gain exposure to the crypto market.

The analysis seeks to determine whether these new ETFs serve as a portfolio diversification option, act as a safe haven during market turbulence, or move in sync with established markets—a question of interest to various market participants aiming to invest in these instruments for protection or speculation. To achieve this objective, models based on vine copulas will be employed, which are particularly well suited for modeling dependence across many variables.

The paper comprises five additional sections beyond this introduction. The theoretical framework (Section 2) presents studies on cryptocurrencies and dependence analysis among financial assets. Section 3 outlines the methodological procedures used in this work. Section 4 describes the data set employed. Section 5 discusses the results obtained. Finally, the concluding remarks are delivered in Section 6.

2. Theoretical Framework

Bitcoin was presented in a paper by Nakamoto (2008), launched the following year, and its first official exchange rate was 1,006 bitcoins per US dollar (Burniske and Tatar, 2017; Jeegers, 2023). The fundamental idea was to create a decentralized, peer-to-peer (P2P) payment system whose transactions are recorded and validated in a public database known as the blockchain.

Since then, other crypto-assets have emerged to serve different purposes. Burniske and Tatar (2017) divides these assets into three categories: (i) cryptocurrencies, which are cryptographically secured digital currencies that can be exchanged over a network; (ii) cryptocommodities, digital resources that can be used as inputs for a final digital good; (iii) tokens (or cryptotokens), final digital goods or services.

After Bitcoin, the second most popular crypto-asset is Ethereum, which was launched by Buterin et al. (2014). Although inspired by its predecessor, its operation is quite different. Ethereum functions as a platform that allows users to develop decentralized applications (dApps) and to craft *smart contracts* (Burniske and Tatar, 2017). Thus, it can be classified in the category of *cryptocommodity*. Additionally, Ethereum has a cryptocurrency, Ether, which operates similarly to Bitcoin.

According to [Statista \(2023\)](#), there are currently around 9,000 different cryptocurrencies, each with distinct purposes and functionalities. However, many of these projects prove to be fraudulent, serving illicit ends such as money laundering, extortion, or Ponzi schemes ([Bartoletti et al., 2021](#)).

Several studies have been conducted to analyze the behavior and distinct characteristics of these financial instruments. These analyses have focused not only on the singularities of this asset class but also on how they align with or diverge from more traditional market investment options. In general, cryptocurrency returns are leptokurtic; their autocorrelations decay rapidly, there are volatility clusters and strong leverage effects, as well as long-range dependence in both volatility and returns and a correlation between price and volume ([Gebka and Wohar, 2013](#); [Zhang et al., 2018](#); [Bouri et al., 2019](#)).

[Gadi and Sicilia \(2022\)](#) analyze the hedge and diversification properties of various cryptocurrencies compared to major global market indices. Covering the period from 2018 to 2022, the study employs the model of [Baur and McDermott \(2010\)](#) to assess the behavior of these assets in comparison to the G7 and BRICS markets, with a focus on the changes brought about by the COVID-19 pandemic. The study reveals that, during the pandemic, gold lost its hedging properties. At the same time, some stablecoins¹ remained effective for most markets. Bitcoin, which had previously served as a hedging instrument, became a diversifier after the crisis. Other cryptocurrencies, such as Ethereum, Litecoin, and BitcoinCash, have also emerged as diversifiers.

[Yi et al. \(2018\)](#) and [Charfeddine et al. \(2022\)](#) examine the volatility linkages in the crypto-asset market. In the first study, they point out that cryptocurrencies with larger market capitalizations do not always act as volatility transmitters, whereas smaller ones tend to be volatility receivers. In the second one, the analysis is based on different classes of these assets, which are divided into three types: mined coins, non-mined coins, and tokens. The authors demonstrate that there is generally strong dependence in this market and that mined coins exert contagion effects on the other two classes, with Ethereum influencing all of them. Non-mined coins and tokens show low interdependence, suggesting that investing in these two segments may offer a viable diversification strategy.

Modeling the dependence between financial assets is critical for improving risk management and portfolio allocations, as it facilitates the development of investment strategies that offer greater protection against tail events. In general, many studies and models employ the Pearson correlation coefficient to measure the association between different financial instruments. However, this measure

¹These are cryptocurrencies with price stabilization mechanisms ([Mita et al., 2019](#)).

captures only the linear relationship between variables, which can be a limiting factor, given that financial series typically exhibit non-linear associations due to being leptokurtic and asymmetric (Poon et al., 2004; Hu, 2006; Huang et al., 2009). Therefore, it is necessary to employ other approaches that are more flexible and better suited to handling financial data; one such methodology is the copula theory, which will be adopted in this work.

Boako et al. (2019) examine the dependence relationships and the value-at-risk (VaR) of a portfolio composed of five cryptocurrencies—Bitcoin, Dash, Ethereum, Litecoin, Ripple, and Stellar—using R-Vine copulas. According to the authors, Ethereum offers the best risk-return trade-off. Furthermore, a strong dependence was found between Bitcoin and Ethereum, whereas the other crypto-assets exhibited low interdependence among themselves but somewhat higher association with Bitcoin.

Jeribi and Fakhfekh (2021) analyze the relationship between five cryptocurrencies, Bitcoin, Dash, Monero, Ethereum, and Ripple, oil prices (WTI), and the S&P500 and NASDAQ indices. The objective is to identify the optimal hedging strategy for a portfolio composed of these assets based on results obtained from estimating a FIEGARCH model, an extreme-value copula model, and a hedge ratio analysis. The data cover the period from January 2016 to November 2019. The results show a negative and significant leverage effect in the returns of the U.S. indices and WTI, while cryptocurrency markets exhibit a positive asymmetric volatility effect. Furthermore, the dependence in the bivariate copulas is very weak. The authors suggest that investors should hold a greater proportion of conventional financial assets in their portfolios than digital ones.

In Osman et al. (2023), an analysis is conducted on diversification strategies that combine traditional assets and cryptocurrencies using the R-Vine model, along with the Mean-CVaR portfolio optimization model. The results suggest that cryptocurrencies can serve as a weak hedge or a safe haven against market indices in certain situations. Moreover, the study suggests that when including Bitcoin and Ethereum in a portfolio, adding the S&P 500 may not be particularly attractive from a risk perspective.

3. Methodology

This work adopts two methodologies for modeling the dependence structure among the selected financial assets. The first concerns the estimation of marginal distributions, and the second refers to the estimation of *vine* copula models. A generalized autoregressive conditional heteroscedasticity (GARCH) model is employed for the first part. This family of models is chosen so

that a filtered inference of the marginal functions of the financial assets can be performed. The second part uses the *Pair-Copula Construction* approach developed by [Bedford and Cooke \(2002\)](#).

3.1 Modeling and Extracting the Marginals

The estimated model is based on GARCH family models introduced by [Bollerslev \(1986\)](#). Let r_t be a stationary time series representing an asset's return, with mean μ . Then it can be expressed as follows:

$$r_t = \mu + \xi_t \quad (1)$$

$$\xi_t = \sigma u_t, \quad u_t \stackrel{i.i.d.}{\sim} (0,1) \quad (2)$$

$$\sigma^2 = \omega + \sum_{i=1}^q \alpha_i \xi_{t-i}^2 + \sum_{j=1}^p \beta_j \sigma_{t-j}^2 \quad (3)$$

where ξ_t are the error terms, u_t is white noise, $\omega > 0$, $\alpha_i \geq 0$, $i = 1, \dots, q$ and $\beta_j \geq 0$, $j = 1, \dots, p$. The GARCH model has some limitations: positive and negative returns are treated symmetrically in terms of volatility, yet financial series tend to react more strongly to adverse shocks than to positive ones. Moreover, its parameters must always be positive to ensure that the conditional volatility remains positive, and this restriction can complicate model estimation ([Nelson, 1991](#)). In light of this issue, [Nelson \(1991\)](#) proposed a model that overcomes these limitations, the exponential GARCH (EGARCH). The EGARCH,(p,q) model can be defined as:

$$\ln(\sigma_t^2) = \omega + \sum_{j=1}^p \beta_j \ln(\sigma_{t-j}^2) + \sum_{j=1}^q (\alpha_j u_{t-j} + \gamma_j (|u_{t-j}| - \mathbb{E}|u_{t-j}|)) \quad (4)$$

The parameter γ captures the asymmetry in shock impact: when $\gamma = 0$, positive and negative shocks affect volatility equally. The parameters may be non-positive because variance enters the model via a logarithm.

The estimation of GARCH family models is used to infer the marginal functions, as proposed in the works of [Shih and Louis \(1995\)](#) and [Joe and](#)

Xu (1996). This approach involves separately estimating the parameters of the marginal distributions, followed by estimating a copula function that is conditional on the estimates from the volatility model (Liu and Luger, 2009). Additionally, the GARCH model acts as a filter that eliminates serial dependence. Consequently, the copula model can be estimated based on the independent and identically distributed residuals obtained after this filtering (Brechmann and Joe, 2015).

After estimating the univariate models, the residuals are extracted and standardized, that is:

$$\xi_t = \frac{r_t - \hat{\mu}_t}{\hat{\sigma}^2} \quad (5)$$

Then, this matrix of standardized residuals is transformed into pseudo-observations as proposed by Berg and Aas (2009), which will be used to model the dependence structure in the copula model.

3.2 Copula Theory

To analyze the dependence structure among the selected financial assets, we apply the concept of copulas, which are functions that connect univariate marginal distributions to their multivariate distribution. According to Kolev et al. (2006), the formal definition of copulas is:

Definition 1 (Formal Definition of Copulas). An n -dimensional copula function is a function $C : [0,1]^n \rightarrow [0,1]$ that satisfies the following properties:

1. Groundedness: for every $\mathbf{s} = (s_1, \dots, s_n) \in [0,1]^n$, $C(\mathbf{s}) = 0$ if at least one coordinate $s_i = 0$.
2. $C(s_1, \dots, s_n)$ is n -increasing.
3. $C(1, \dots, 1, s_i, 1, \dots, 1) = s_i \forall s_i \in [0,1], i = 1, \dots, n$.

A informal definition provided by Mai and Scherer (2014) is:

Definition 2 (Informal Definition of Copulas). A function $C : [0,1]^n \rightarrow [0,1]$ is called a copula if there exists a random vector (S_1, \dots, S_N) such that each component S_k has a uniform marginal distribution on $[0,1]$ for $k = 1, \dots, n$ and

$$C(s_1, \dots, s_n) = \mathbb{P}(S_1 \leq s_1, \dots, S_n \leq s_n), s_1, \dots, s_n \in [0,1].$$

In this study, the random vector $S = (S_1, \dots, S_N)$ is defined as the vectors of standardized residuals derived from the univariate GARCH models applied to the selected financial assets. These residuals are then transformed into pseudo-observations uniformly distributed on the interval $[0,1]$. The definition of a copula is based on Sklar's theorem (Sklar, 1959), which marks the starting point of copula theory.

Theorem 1 (Sklar's Theorem). Let S be an n -dimensional random vector with joint distribution function H and marginal distribution functions H_i for $i = 1, \dots, n$. Then the joint distribution function can be expressed as follows:

$$H(s_1, \dots, s_n) = C(H_1(s_1), \dots, H_n(s_n)) \quad (6)$$

where C is an n -dimensional copula. For absolutely continuous distributions, the copula C is unique.

Proof. See Nelsen (2006) or McNeil et al. (2015). ■

According to Czado (2019), from Theorem 1, the probability density function or probability mass function is given by

$$h(s_1, \dots, s_n) = c(H_1(s_1), \dots, H_n(s_n)) h_1(s_1) \cdots h_n(s_n) \quad (7)$$

for some n -dimensional copula C with copula density c .

The converse is also true, the copula corresponding to a multivariate distribution H with marginal distributions H_i , for $i = 1, \dots, n$, can be represented as

$$C(s_1, \dots, s_n) = H(H_1^{-1}(s_1), \dots, H_n^{-1}(s_n)) \quad (8)$$

and its copula density or probability mass function is determined by

$$c(s_1, \dots, s_n) = \frac{h(H_1^{-1}(s_1), \dots, H_n^{-1}(s_n))}{h_1(H_1^{-1}(s_1)) \cdots h_n(H_n^{-1}(u_n))}. \quad (9)$$

The main applications of Sklar's theorem are the estimation of dependence between standardized variables and the construction of multivariate distributions (Kolev et al., 2006; McNeil et al., 2015; Czado, 2019).

Another important concept to establish when discussing copulas is the Fréchet-Hoeffding bounds.

Theorem 2 (Fréchet-Hoeffding Bounds). Every copula $C(s_1, \dots, s_n)$ satisfies the following inequality:

$$W^n(\mathbf{s}) \leq C(\mathbf{s}) \leq M^n(\mathbf{s}) \quad (10)$$

where $\mathbf{s} = (s_1, \dots, s_n)$, $W^n(\mathbf{s}) = \max(\sum_{i=1}^n s_i + 1 - n, 0)$ e $M^n(\mathbf{s}) = \min(s_1, \dots, s_n)$.

The lower bound and the upper bound are given by $W(s_1, \dots, s_n)$ and $M(s_1, \dots, s_n)$, respectively.

3.2.1 Dependence Measures

Since copulas measure the dependence structure between random variables, we will explore important measures of association for the analysis presented in this work.

Definition 3 (Pearson correlation coefficient). Let X and Y be any two random variables, their correlation coefficient is given by:

$$\rho(X, Y) = \frac{\text{cov}(X, Y)}{\sqrt{\text{var}(X)\text{var}(Y)}} \quad (11)$$

The correlation coefficient, ρ , ranges between $[-1, 1]$. Values closer to zero indicate a weak relationship between the variables. The correlation is positive when $\rho > 0$; conversely, if $\rho < 0$, the correlation is negative. It is important to emphasize that this coefficient measures only linear relationships, which can be problematic when modeling financial time series since these are typically leptokurtic and asymmetric, which may imply nonlinear dependencies (Huang et al., 2009).

Another measure of association is Kendall's τ , which is based on the number of concordant and discordant pairs of observations. Consider a random vector (X_1, Y_1) and a second vector with the same distribution but independent of the first, $(\check{X}_1, \check{Y}_1)$. These vectors are concordant if $(X_1 - \check{X}_1)(Y_1 - \check{Y}_1) > 0$ and discordant if $(X_1 - \check{X}_1)(Y_1 - \check{Y}_1) < 0$ (Nelsen, 2006; Czado, 2019)

Definition 4 (Kendall's Tau). The Kendall's τ between the random vectors (X_1, Y_1) and $(\check{X}_1, \check{Y}_1)$ is defined as

$$\tau(X_1, Y_1) = P\{(X_1 - \check{X}_1)(Y_1 - \check{Y}_1) > 0\} - P\{(X_1 - \check{X}_1)(Y_1 - \check{Y}_1) < 0\}. \quad (12)$$

Another important concept is tail dependence, which measures the dependence between pairs of random variables based on their continuous marginal

distributions. It is captured by two coefficients, upper and lower, focusing specifically on dependence in the tails of bivariate distributions, providing insight into the strength of this relationship in extreme events. Moreover, these coefficients are defined as conditional probabilities exceeding high quantiles (McNeil et al., 2015).

Definition 5 (Coefficients of Tail Dependence). The upper tail dependence coefficient of a bivariate distribution with copula C is defined as:

$$\lambda_{u_i} = \lim_{q \rightarrow 1^-} P(X_2 > H_2^{-1}(q) | X_1 > H_1^{-1}(q)) = \lim_{q \rightarrow 1^-} \frac{1 - 2q + C(q, q)}{1 - q}, \quad (13)$$

And the lower tail dependence coefficient is:

$$\lambda_{l_i} = \lim_{q \rightarrow 0^+} P(X_2 \leq H_2^{-1}(q) | X_1 \leq H_1^{-1}(q)) = \lim_{q \rightarrow 0^+} \frac{C(q, q)}{q} \quad (14)$$

This work follows the definitions presented in Talbi et al. (2021) and Osman et al. (2023). An asset is considered a *strong hedge* when the association, measured by Kendall's τ , is negative, and a *weak hedge* when it is equal to or close to zero. Furthermore, it is a *weak safe haven* when the lower tail dependence coefficient, λ_{l_i} , is zero, and a *strong safe haven* when $\lambda_{l_i} = 0$ and $\tau < 0$.

3.2.2 Copula Families

Based on Theorem 1, we can model different copulas to represent the relationship between sets of variables. Table 1 shows the copulas used in this work.

Table 1
Copula Families and Their Mathematical Description

Name	Functional Form	Parameter Range	Tail Dependence
Independence	$\prod (s_1, \dots, s_n) = \prod_{i=1}^n s_i$	-	-
Gaussian	$C_R^N(s_1, \dots, s_n) = \Phi_R(\Phi^{-1}(s_1), \dots, \Phi^{-1}(s_n))$	$R \in [-1, 1]$	-
t	$C_{R, \nu}^t(s_1, \dots, s_n) = \frac{1}{\sqrt{\det R}} \frac{\Gamma(\frac{\nu+1}{2}) \Gamma(\frac{\nu}{2})^n}{[\Gamma(\frac{\nu+1}{2})]^\nu} \frac{\prod_{k=1}^n (1 + \frac{s_k^2}{\nu})^{\frac{\nu-1}{2}}}{(1 + \frac{\sum_{k=1}^n s_k^2}{\nu})^{\frac{\nu+n}{2}}}$	$R \in [-1, 1], \nu > 2$	Upper and Lower
Clayton	$C_\theta^C(s_1, \dots, s_n) = (\sum_{k=1}^n s_k^{-\theta} - n + 1)^{-\frac{1}{\theta}}$	$\theta \in (0, \infty)$	Upper
Gumbel	$C_\theta^G(s_1, \dots, s_n) = \exp\left(-\left(\sum_{k=1}^n (-\ln s_k)^\theta\right)^{1/\theta}\right)$	$[1, \infty)$	Upper
Frank	$C_\theta^F(s_1, \dots, s_n) = -\frac{1}{\theta} \ln\left(1 + \frac{\prod_i (\exp(-\theta s_i) - 1)}{\exp(-\theta) - 1}\right)$	$\theta \in [-\infty, \infty]$	Upper and Lower
Joe	$C_\theta^J(s_1, \dots, s_n) = 1 - \left(1 - \left[1 - (1 - s_1)^\theta\right] \dots \left[1 - (1 - s_n)^\theta\right]\right)^{1/\theta}$	$\theta \in [1, \infty)$	Upper

3.3 Vine Copulas

In theory, estimating a multivariate copula is feasible; however, when working with high-dimensional variables, this approach can prove inflexible due to the limitation in the number of parameters and the lack of equivalence in tail dependence. For example, the Gaussian copula cannot capture tail dependence in the distribution. On the other hand, the Student's t copula has only a single parameter for the degrees of freedom, which becomes a limitation when dealing with a large set of variables. When extended to a multivariate framework, Archimedean copulas require additional constraints on the estimated parameters, reducing flexibility in modeling the dependency structure (Czado, 2010; Joe and Kurowicka, 2011; Czado, 2019).

Bedford and Cooke (2002) introduced an approach called Pair-Copula Constructions (PCC) based on decomposing multivariate distributions into bivariate copulas via blocks. The structure of the PCC is illustrated through vines, a graphical representation that encodes the dependency structure and its construction.

The PCC approach is based on the decomposition of n -dimensional density functions. Consider a vector of random variables $S = (S_1, \dots, S_n)$ with joint density function $h(s_1, \dots, s_n)$. This function can be factored as follows:

$$h(s_1, \dots, s_n) = h_n(s_1) \cdot h(s_{n-1}|s_n) \cdot h(s_{n-2}|s_{n-1}, s_n) \cdots h(s_1|s_2, \dots, s_n) \quad (15)$$

From equation 7 of Sklar's theorem, the bivariate joint density function can be expressed as:

$$h(s_1, s_2) = c_{12}(H_1(s_1), H_2(s_2)) \cdot h_1(s_1) \cdot h_2(s_2) \quad (16)$$

where $c_{12}(H_1(s_1), H_2(s_2))$ is the density of this pair-copula for the variables $H_1(s_1)$ and $H_2(s_2)$. The conditional density is then given by:

$$h(s_1|s_2) = c_{12}(H_1(s_1), H_2(s_2)) \cdot h_1(s_1) \quad (17)$$

Similarly, for the case of three random variables, we have:

$$h(s_1|s_2, s_3) = c_{12|3}(H(s_1|s_2), H(s_2|s_3)) \cdot h(s_1|s_3) \quad (18)$$

or

$$h(s_1|s_2, s_3) = c_{13|2}(H(s_1|s_2), H(s_2|s_3)) \cdot h(s_1|s_2) \quad (19)$$

where $c_{12|3}$ and $c_{13|2}$ are, respectively, the density of the copula of variables 1 and 2 conditional on 3, and the density of the copula of variables 1 and 3 conditional on 2. One can then generalize this decomposition as follows:

$$h(s|\boldsymbol{\kappa}) = c_{sk_j|\boldsymbol{\kappa}_{-j}}(H(s|\boldsymbol{\kappa}_{-j}), H(k_j|\boldsymbol{\kappa}_{-j})) \cdot h(s|\boldsymbol{\kappa}_{-j}) \quad (20)$$

Let $\boldsymbol{\kappa}$ be an n -dimensional vector, k_j an arbitrary component of $\boldsymbol{\kappa}$, and let $\boldsymbol{\kappa}_{-j}$ denote the vector $\boldsymbol{\kappa}$ without this component. Thus, it follows that, under the conditions outlined above, a multivariate density can be expressed as a product of *pair-copulas*. This construction is iterative, and numerous possible ways exist to construct these pair-copulas given a specific factorization (Aas et al., 2009).

To compute the density in equation (20), an expression for the conditional distribution function $H(s|\boldsymbol{\kappa})$ is required. According to Joe (1996), for every j , we have:

$$H(s|\boldsymbol{\kappa}) = \frac{\partial C_{s,k_j|\boldsymbol{\kappa}_{-j}}(H(s|\boldsymbol{\kappa}_{-j}), H(k_j|\boldsymbol{\kappa}_{-j}))}{\partial H(k_j|\boldsymbol{\kappa}_{-j})} \quad (21)$$

where $C_{s,k_j|\boldsymbol{\kappa}_{-j}}$ is the distribution function of a bivariate copula.

3.3.1 Regular Vines

PCC modeling occurs via the decomposition of multivariate densities into $n(n-1)/2$ bivariate copula densities for $n > 2$. Graphical models representing this construction are called vines. There are three classes of vine copulas used in this work: *Regular Vine* (R-Vine), *Canonical Vine* (C-Vine), and *Drawable Vine* (D-Vine).

According to Cooke et al. (2010), a vine \mathcal{V} on n variables is a nested set² of connected trees $\mathcal{V} = (T_1, \dots, T_{n-1})$ if and only if the edges of tree j are the nodes of tree $j+1$, for $j = 1, \dots, n-2$. A regular vine on n variables is a vine whose two edges in tree j are connected by an edge in tree $j+1$ only if they share a common node; formally:

²A nested set is a collection of sets that consists of chains of subsets forming a hierarchical structure.

Definition 6 (Regular Vines). \mathcal{V} is a Regular Vine (R-Vine) on n elements, where $E(\mathcal{V}) = E_1 \cup \dots \cup E_{n-1}$ denotes the set of edges of \mathcal{V} if:

1. $\mathcal{V} = (T_1, \dots, T_{n-1})$;
2. T_1 is a connected tree with nodes $N_1 = \{1, \dots, n\}$ and edges E_1 . For $i = 1, \dots, n-1$, T_i is the tree with nodes $N_i = E_{i-1}$;
3. For $i = 2, \dots, n-1$ $e \{a, b\} \in E_i$, with $a = \{a_1, a_2\}$ e $b = \{b_1, b_2\}$, then $\#|a \cap b| = 1$ (Proximity Condition).

Bedford and Cooke (2002) identified two exceptional cases of regular vines. A regular vine is called *C-Vine* if each tree T_i has a single node with $n-1$ edges, this node is called the root; *D-Vine* if each node in T_i has at most two edges.

There are three sets associated with the edges of a regular vine. An edge's *complete union* (U_{e_i}) is the set of all indices that the edge contains. If two nodes a and b are connected by an edge, then the *conditioned set* ($C_{e_i, a}$) and the *conditioning set* (D_{e_i}) of this edge are, respectively, the symmetric difference and the intersection of the complete unions of a and b .

To construct an R-Vine copula, it is necessary to specify $n-1$ unconditional bivariate copulas among variables indexed by the conditioned sets of the edges in the first tree of the R-Vine. For the second tree of the R-Vine, one must specify the bivariate copulas among variables indexed by the conditioned sets conditional on variables indexed by the conditioning sets of the edges of the R-Vine (Dißmann et al., 2013). Thus, we can define what an R-Vine copula specification is.

Definition 7 (R-Vine Copula Specification). (H, \mathcal{V}, B) is a R-Vine copula specification if $H = (H_1, \dots, H_n)$ is a vector of continuous, invertible distribution functions, \mathcal{V} is an n -dimensional R-Vine, and $B = \{B_e | i = 1, \dots, n-1; e \in E_{ij}\}$ is a set of copulas, with each B_e being a pair-copula.

We can now calculate our *vines* densities

Theorem 3 (R-Vine Density). Let (H, \mathcal{V}, B) be an R-Vine copula specification on n elements, then there exists a unique distribution H that realizes this R-Vine copula specification, with density:

$$h_{1\dots n}(s) = \prod_{k=1}^n h_k(s_k) \prod_{i=1}^{n-1} \prod_{e \in E_i} c_{C_{e,a}, C_{e,b} | D_e} \left(H_{C_{e,a} | D_e} (s_{C_{e,a}} | \mathbf{s}_{D_e}), H_{C_{e,b} | D_e} (s_{C_{e,b}} | \mathbf{s}_{D_e}) \right) \quad (22)$$

where $s = (s_1, \dots, s_n)$, $e = \{a, b\}$ denotes the variables in D_e , i.e., $s_{D_e} = \{s_i | i \in D_e\}$. h_i denotes the density of H_i for $i = 1, \dots, n$.

Theorem 4 (C-Vine Density).

$$h(s_1, \dots, s_n) = \left[\prod_{j=1}^{n-1} \prod_{i=1}^{n-j} c_{j, j+i; 1, \dots, j-1} \right] \cdot \left[\prod_{k=1}^n h_k(s_k) \right] \quad (23)$$

Theorem 5 (D-Vine Density).

$$h_{1, \dots, n}(s_1, \dots, s_n) = \left[\prod_{j=1}^{n-1} \prod_{i=1}^{n-j} c_{i, (i+j); (i+1), \dots, (i+j-1)} \right] \cdot \left[\prod_{k=1}^n h_k(s_k) \right] \quad (24)$$

A difficulty when working with vines is finding the best structure that will fit the dataset, i.e., choosing the pair-copulas that will compose the trees to be estimated most accurately. This is especially true when working with R-Vines, because whereas in C-Vines and D-Vines, the number of possible structures is given by $\frac{n!}{2}$, [Morales-Napoles \(2010\)](#) showed that for an R-Vine this number is given by $\frac{n!}{2} \cdot 2^{\binom{n-2}{2}}$.

We use the algorithm proposed by [Dißmann et al. \(2013\)](#) to construct the structure of an R-Vine, aiming to identify the structure that captures the highest dependence in the copula pairs of the first tree. The selection criterion is the tree that maximizes the sum of the absolute values of Kendall's τ for its set of bivariate copulas. It is worth noting that this approach applies a truncation to the R-Vine specification, assuming independence in the last k trees to reduce the number of parameters, as proposed by [Brechmann et al. \(2012\)](#). For a C-Vine, we can adapt the algorithm to select the node with the greatest dependence among all other nodes, that is, to select a root node. In the case of a D-Vine, since we seek to find the path that traverses the dependency structure, it becomes necessary to adapt the solution to find a Hamiltonian path³, which is equivalent to solving a Traveling Salesman Problem⁴, which can be a somewhat inefficient strategy when working with very high dimensions ([Dißmann et al., 2013](#)).

It is also necessary to select the copula, among those presented in 3.2.2, that best fits each pair-copulas. A maximum likelihood estimation is performed for each candidate copula, and the one with the lowest Bayesian Information Criterion (BIC) is chosen ([Dißmann et al., 2013](#)).

³A path that visits each vertex of a graph only once ([Czado, 2019](#)).

⁴In this problem, we seek to determine the shortest route that visits each node and returns to the starting node ([Czado, 2019](#)).

After determining each pair-copula's structure and family, the next step is to estimate their parameters via a log-likelihood function. To this end, let $s^{(1)}, \dots, s^{(d)}$ be an i.i.d. sample of size d from an n -dimensional R-Vine copula specified by (H, \mathcal{V}, B) , and let equation (22) denote its density. The log-likelihood of the R-Vine is then given by

$$\ell(\boldsymbol{\theta}; \mathbf{s}) = \prod_{k=1}^d \prod_{j=1}^{n-1} \prod_{e \in E_j} \log [c_{a_e, b_e; D_e} (C_{a_e | D_e} (s_{k, a_e} | \mathbf{s}_{k, D_e}), C_{b_e | D_e} (s_{k, b_e} | \mathbf{s}_{k, D_e}))], \quad (25)$$

From equations (23) and (24), the log-likelihoods of a C-Vine and a D-Vine are expressed, respectively, as:

$$\ell(\boldsymbol{\theta}, \mathbf{s}) = \prod_{k=1}^d \prod_{j=1}^{n-1} \prod_{i=1}^{n-j} \log [c_{j, i+j; 1:j-1} (C_{i|1:j-1} (s_{k, i} | \mathbf{s}_{k, 1:j-1}), C_{i+j|1:j-1} (s_{k, i+j} | \mathbf{s}_{k, 1:j-1}))], \quad (26)$$

$$\ell(\boldsymbol{\theta}, \mathbf{s}) = \prod_{k=1}^d \prod_{j=1}^{n-1} \prod_{i=1}^{n-j} \log [c_{i, i+j; i+1:i+j-1} (C_{i|i+1:i+j-1} (s_{k, i} | \mathbf{s}_{k, i+1:i+j-1}), C_{i+j|i+1:i+j-1} (s_{k, i+j} | \mathbf{s}_{k, i+1:i+j-1}))], \quad (27)$$

The goodness-of-fit test used in this study is proposed by [Genest et al. \(2009\)](#). This test is based on transforming the data using the probability integral transform (PIT). It aims to compute the distance between the empirical copula of the transformed data, obtained by the procedures explained in the previous sections, and the independence copula. The test can be performed using a Cramér–von Mises (CvM) statistic or a Kolmogorov–Smirnov (KS) statistic. The test's null hypothesis is that the vine copula model is well-fitted. The tests proposed by [Vuong \(1989\)](#) and [Clarke \(2007\)](#) were conducted to compare the estimated vines models.

4. Data

The dataset comprises the log-returns of the ETFs BOVA11, EURP11, GOLD11, HASH11, IVVB11, QBTC11, QETH11, XINA11, TIP, and SHY

and was retrieved from [Yahoo Finance \(2024\)](#). The time series spans from August 5, 2021, to August 25, 2023. This interval begins one day after the launch of QETH11 and includes 500 observations. The assets selected for this study were chosen based on their relevance and representativeness in the market. The HASH11, QBTC11, and QETH11 funds were the first cryptocurrency ETFs launched in the Brazilian market. In contrast, BOVA11, EURP11, IVVB11, and XINA11 are more traditional investment alternatives, representing market indices. Additionally, GOLD11, TIP, and SHY were included because they represent investment options considered safer, i.e., gold, short-term U.S. bonds, and inflation-linked U.S. bonds, providing investors with a means to protect their portfolios against market volatility and uncertainty ([Baur and McDermott, 2016](#)). Table 2 presents the details of the selected funds and Figure 2 in Appendix B shows the corresponding time series.

Table 3 presents the descriptive statistics of the returns of the analyzed assets and the results of the unit root tests. All assets exhibited, on average, a negative change over the period and displayed skewness. They are leptokurtic, except for QBTC11, GOLD11, BOVA11, and TIP. Moreover, the null hypothesis of normality is rejected by the Jarque–Bera test for all assets except BOVA11. The highest positive logarithmic return was observed for XINA11, followed by HASH11. The most significant decline occurred for QETH11, with HASH11 ranking second. The most volatile assets were QETH11, followed by HASH11, while SHY and TIP were the least volatile. According to the results of the unit root tests, the log returns of the selected financial assets are stationary.

Table 2
Selected ETFs, their benchmark indices, and manager

Ticker	Benchmark Index	Manager
HASH11	Nasdaq Crypto Index	Hashdex
QBTC11	CME CF Bitcoin Reference Rate	QR Capital
QETH11	CME CF Ether Reference Rate	QR Capital
GOLD11	LBMA Gold Price	XP Asset
IVVB11	S&P 500 Brazilian Real Index	BlackRock
BOVA11	Ibovespa B3	BlackRock
EURP11	MSCI Europe Investable Market	XP Asset
XINA11	MSCI China	XP Asset
TIP	ICE US Treasury Inflation Linked Bond Index (USD)	BlackRock
SHY	ICE US Treasury 1–3 Year Bond Index	BlackRock

Source: Prepared by the authors.

Table 3
Descriptive statistics and unit root tests

	HASH11	QBTC11	QETH11	GOLD11	IVVB11	BOVA11	EURP11	XINA11	TIP	SHY
Descriptive statistics										
Mean	-0.001	-0.001	-0.002	-0.0002	-0.0001	-0.00004	-0.0003	-0.001	-0.0003	-0.0001
Maximum	0.164	0.145	0.146	0.065	0.084	0.054	0.093	0.176	0.018	0.010
Minimum	-0.223	-0.181	-0.291	-0.041	-0.041	-0.040	-0.047	-0.086	-0.017	-0.005
Std. Dev.	0.037	0.036	0.045	0.012	0.013	0.013	0.014	0.022	0.005	0.002
Skewness	-0.398	-0.109	-0.641	0.325	0.554	-0.061	0.629	1.207	0.241	0.811
Kurtosis	3.867	2.308	4.425	2.035	3.085	0.307	4.748	9.103	1.194	5.994
Jarque-Bera	329.319	122.928	447.813	96.883	227.240	2.450	508.967	1.867.119	35.431	602.727
Probability	0.00000	0.00000	0.00000	0.00000	0.00000	0.294	0.00000	0.00000	0.00000	0.00000
Unit root tests										
ADF test	-7.40**	-7.69**	-7.22**	-8.97**	-8.68**	-7.72**	-9.13**	-7.61**	-7.65**	-7.91**
PP test	-458.72**	-468.29**	-442.70**	-451.42**	-454.26**	-492.21**	-475.23**	-508.62**	-454.82**	-476.38**
KPSS test	0.14	0.14	0.11	0.04	0.07	0.13	0.10	0.07	0.12	0.37
ERS test	-5.27***	-4.95***	-4.45***	-10.65***	-5.18***	-10.49***	-5.18***	-9.40***	-5.08***	-8.28***

Note: $+p < .10$, $*p < .05$, $**p < .01$, $***p < .001$.

5. Results

The EGARCH (1,1) specification was utilized for the marginal modeling, as it offered the best fit for most of the analyzed assets. The model innovations were assumed to follow a Student's t distribution. These choices were made because they resulted in the lowest Bayesian Information Criterion (BIC). The findings are presented in Table 4.

Table 4
EGARCH model estimation

	HASH11	QBTC11	QETH11	GOLD11	IVVB11	BOVA11	EURP11	XINA11	TIP	SHY
Parameters										
μ	-0.000945	-0.001409	-0.001574	-0.000231	-0.000119	-0.000001	-0.000652	-0.002259**	-0.000249	-0.000083
ω	-0.069409**	-0.002637	-0.069741***	-0.396112***	-0.070108***	-0.469645***	-0.188039***	-0.082876***	-0.928567***	-0.295511***
α	-0.018747	-0.004144	-0.029937	0.037244	-0.042200*	-0.069453**	-0.050473*	-0.080347***	-0.032441	-0.004388
β	0.990197***	1.000000**	0.989408***	0.956014***	0.992211***	0.945760***	0.978461***	0.989138***	0.913047***	0.977010***
γ	0.112446	0.059572***	0.074818**	0.116423***	0.078226***	0.045122	0.128676***	0.082060***	0.288762***	0.327117***
Shape	4.723134***	5.011540***	6.392908***	9.782144*	19.40303	29.90982	8.615565	9.447447	7.976666	3.807549*
Validation tests										
Q(5)	3.435	2.7089	1.7286	7.387*	5.1626	0.89969	2.290	1.740	9.977362**	3.126
Q ² (5)	6.176*	5.963*	3.680	7.108*	2.172	2.416	1.092	5.16194	1.06037	6.369
ARCH-LM(5)	0.8673	0.2513	0.638837	0.05484	3.34647	1.464	1.0368	6.313*	2.5056	2.126

Note: $+p < .10$, $*p < .05$, $**p < .01$, $***p < .001$.

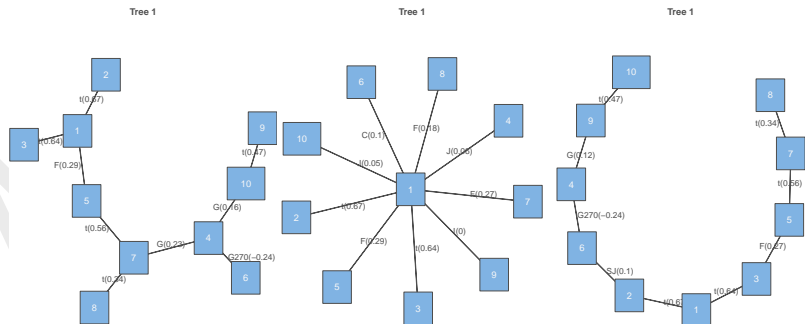
Except for XINA11, the mean of the log-returns, μ , was not significantly different from zero for any of the assets analyzed at the 5% significance level. The parameter ω was negative for all series, although it was not significant for QBTC11. The asymmetric effects of shocks on volatility are measured by the parameter α . This parameter is not significant at the 5% level for the majority of the ETFs analyzed, except for IVVB11, BOVA11, and XINA11, while EURP11 was significant only at the 10% level, which indicates the presence of leverage effects in these assets. The parameter β measures the persistence of volatility and is significant in all estimated models. The results obtained present values very close to 1, indicating that this volatility's effects are long-lasting for all ETFs analyzed.

The magnitude of the shocks is measured by the parameter γ . This pa-

parameter was not significant for HASH11 and BOVA11, which may indicate that negative and positive shocks have similar effects on volatility. Conversely, positive values were found for the other ETFs, indicating that adverse shocks increase the volatility of returns. The weighted Ljung–Box test results suggest the absence of serial correlation in the residuals of most of the estimated models at five lags, except for GOLD11 and TIP. On the other hand, for the squared residuals at five lags, the null hypothesis is rejected only for GOLD11 at the 5% significance level. For the ARCH–LM test with five lags, the null hypothesis of correct ARCH specification is not rejected for the residuals of all models analyzed.

We estimated R-Vine, C-Vine, and D-Vine models to analyze the dependence structure using vine copulas. The families chosen were those specified in sub-subsection 3.2.2. These selections were made to facilitate the application of the test proposed by Genest et al. (2009), which can only be implemented for those copulas families. The estimation and selection method follows the algorithm proposed by Dißmann et al. (2013). In Figure 1, the first trees of each model are presented. These trees best capture the dependence structure among the variables. The values inside the blue boxes represent the financial assets, and the edge labels indicate the copula family and Kendall's tau between each pair of variables.

Figure 1
First tree for R-Vine, C-Vine e D-Vine, respectively



Note: The numbers 1, 2, 3, 4, 5, 6, 7, 8, 9 e 10 are respectively the ETFs: HASH11, QBTC11, QETH11, GOLD11, IVVB11, BOVA11, EURP11, XINA11, TIP and SHY.

In the R-Vine model, the t copula predominated in explaining the relationships among the analyzed assets, especially for the crypto-ETFs. Moreover,

QBTC11 and QETH11 exhibited a strong positive dependence with HASH11, which is expected since Bitcoin and Ethereum have significant weight in this asset's benchmark index. Additionally, HASH11 is weakly and positively related to IVVB11. The Gumbel copula provided the most significant explanatory power among the traditional-asset ETFs. Notably, a negative but low correlation was observed between GOLD11 and BOVA11, which may indicate that gold serves as a hedge against the Brazilian market. [Mensi et al. \(2018\)](#) also found a low positive association using a wavelet-based approach. The European market showed a strong positive relationship with the U.S. market, a moderate one with the Chinese market, and a weak one with gold. Finally, the U.S. inflation and interest-rate-related funds, SHY and TIP, displayed a moderate dependence captured by a t copula.

In the C-Vine estimation, the root asset selected was the HASH11 ETF, which exhibited a low positive correlation with gold and short-term U.S. interest rates, both modeled by a Joe copula. There is independence to the U.S. inflation-linked bond ETF. The asset shows a moderate positive association with IVVB11 and EURP11, captured by a Frank copula, and a weak positive association with the Chinese market, also modeled by a Frank copula. Furthermore, there is a small correlation with the Brazilian market, described by a Clayton copula. As in the R-Vine model, HASH11 was strongly related to the two other cryptocurrency ETFs captured by a t copula.

The dependence structure can be analyzed as a path in the D-Vine model. In this case, a low positive association between the Brazilian market and Bitcoin was captured by a Joe copula rotated by 180° , indicating that Bitcoin may serve as a weak hedge for the Ibovespa. Ethereum (QETH11) and the S&P 500 (IVVB11) exhibited a strong relationship, modeled by a Frank copula, which differs from the result reported by [Osman et al. \(2023\)](#) when analyzing the Ethereum and the index directly. Another low association was found between GOLD11 and TIP, modeled by a Gumbel copula. The relationships of the other asset pairs are identical to those identified in the other models.

Tables 5, 6, and 7 summarize the results obtained from the copula model estimations and their implications for investment strategies are presented. The tables with the full results are in Appendix A. The goodness-of-fit test results for all three models indicate that they are well-fitted according to both the Cramér-von Mises and Kolmogorov-Smirnov criteria.

Table 5
Summary of important results found in the R-Vine model

Tree	Edge	Copula	τ	λ_u	λ_l	Analysis
2	3,2:1	SG	0.12	-	0.16	Weak Hedge ; increased association during extreme downside events
	5,3:1	G	0.05	0.07	-	Weak Hedge; increased association during extreme upside events
	7,1:5	F	0.09	-	-	Weak Hedge
3	5,2:3,1	I	0.00	-	-	Diversification
	7,3:5,1	I	0.00	-	-	Diversification
	8,3:7,5	I	0.00	-	-	Diversification
4	4,1:8,7,5	I	0.00	-	-	Diversification
5	10,1:4,8,7,5	I	0.00	-	-	Diversification
6	6,1:10,4,8,7,5	C	0.08	-	0.02	Weak Hedge; decreased association during extreme downside events
7	9,1:6,10,4,8,7,5	I	0.00	-	-	Diversification

Note: The numbers 1, 2, 3, 4, 5, 6, 7, 8, 9 e 10 are respectively the ETFs:
 HASH11, QBTC11, QETH11, GOLD11, IVVB11, BOVA11, EURP11,
 XINA11, TIP and SHY.

Table 6
Summary of important results found in the C-Vine model

Tree	Edge	Copula	τ	λ_u	λ_l	Analysis
2	7,2:1	I	0.00	-	-	Diversification
	7,3:1	G	0.06	0.08	-	Weak Hedge; increased association during extreme upside events
	7,6:1	G270	-0.08	-	-	Strong safe heaven
	7,9:1	J	0.04	0.10	-	Weak Hedge; increased association during extreme upside events
3	10,7:1	I	0.00	-	-	Diversification
	10,2:7,1	I	0.00	-	-	Diversification
	10,3:7,1	I	0.00	-	-	Diversification
4	6,2:10,7,1	I	0.00	-	-	Diversification
	6,3:10,7,1	I	0.00	-	-	Diversification
5	3,2:6,10,7,1	SG	0.12	-	0.16	Weak Hedge; increased association during extreme downside events
6	3,4:6,10,7,1	I	0.00	-	-	Diversification
	8,2:3,6,10,7,1	I	0.00	-	-	Diversification

Note: The numbers 1, 2, 3, 4, 5, 6, 7, 8, 9 e 10 are respectively the ETFs:
 HASH11, QBTC11, QETH11, GOLD11, IVVB11, BOVA11, EURP11,
 XINA11, TIP and SHY.

Table 7
Summary of important results found in the D-Vine model

Tree	Edge	Copula	τ	λ_u	λ_l	Analysis
2	1,5:3	SG	0.10	-	0.14	Weak Hedge; increased association during extreme downside events
	6,1:2	I	0.00	-	-	Diversification
	4,2:6	G	0.07	0.09	-	Weak Hedge; increased association during extreme upside events
3	1,7:3,5	I	0.00	-	-	Diversification
	2,5:1,3	I	0.00	-	-	Diversification
4	6,5:2,1,3	G90	-0.10	-	-	Strong safe heaven
5	2,8:1,3,5,7	I	0.00	-	-	Diversification
	4,5:6,2,1,3	F	0.18	-	-	Weak Hedge
6	4,7:6,2,1,3,5	G	0.14	0.19	-	Weak Hedge; increased association during extreme upside events
7	4,8:6,2,1,3,5,7	C	0.07	-	0.01	Weak Hedge; decreased association during extreme downside events
8	9,8:4,6,2,1,3,5,7	G90	-0.07	-	-	Strong safe heaven

Note: The numbers 1, 2, 3, 4, 5, 6, 7, 8, 9 e 10 are respectively the ETFs:
 HASH11, QBTC11, QETH11, GOLD11, IVVB11, BOVA11, EURP11,
 XINA11, TIP and SHY.

Table 8 summarizes the fit of the three vine specifications. In the Vuong test, both C-Vine and D-Vine outperform R-Vine, with C-Vine slightly ahead, although none of these differences is significant, even after AIC or BIC penalties. In the Clarke test, C- and D-Vine again beat R-Vine; C-Vine is significantly better at the 5% level under an AIC penalty, but under BIC, there is no significant difference between C-Vine and D-Vine.

Table 8
Comparison tests for the estimated Vines

	Test	Statistic	p-value	Akaike Statistic	Akaike p-value	Schwarz Statistic	Schwarz p-value
Vuong	R-Vine vs. C-Vine	-0.687549	0.491737	-0.499717	0.617274	-0.103899	0.917249
	R-Vine vs. D-Vine	-0.712328	0.476262	-0.594713	0.552035	-0.346863	0.728694
	C-Vine vs. D-Vine	0.113985	0.909250	0.023840	0.980980	-0.166123	0.868060
Clarke	R-Vine vs. C-Vine	219	0.006315	222	0.013826	232	0.117436
	R-Vine vs. D-Vine	238	0.303667	239	0.347664	245	0.687363
	C-Vine vs. D-Vine	252	0.893290	251	0.964335	245	0.687363

6. Concluding Remarks

In recent years, the crypto-assets market has emerged and gained momentum, attracting the interest of institutional investors, researchers, and the general public. Understanding how these assets relate to one another is important for more efficient portfolio management. Due to the complexities involved in investing in these financial instruments, some asset managers have recently begun offering exposure to this market via ETFs. This study aimed to estimate the dependence structure between certain ETFs (HASH11, QBTC11, and QETH11) and others based on traditional assets (GOLD11, IVVB11, BOVA11, EURP11, XINA11, TIP, and SHY). To this end, data from August 2021 through August 2023, consisting of the log returns of these funds, were used. Initially, ten univariate EGARCH models were estimated; their standardized residuals were then extracted, and based on these, three vine copula models (R-vine, C-vine, and D-vine) were fitted. This approach enabled the identification of whether these investment alternatives exhibit hedging, diversification, or safe-haven characteristics relative to conventional allocation strategies.

The results of the goodness-of-fit tests indicate that the estimated models fit the data well, and no significant differences were found among them. The estimates indicate that crypto-asset ETFs are highly interdependent. Furthermore, there is a moderate relationship between the S&P 500 and Bitcoin, as well as between the European indices and HASH11.

In the R-vine estimation, it is observed that QETH11 and QBTC11 exhibit a low association when conditioned on HASH11, suggesting that information

from the conditioning asset can help the development of risk-reduction strategies when incorporating these ETFs into a portfolio. Diversification strategies are indicated by the independence between assets, as in the cases of IVVB11 and QBTC11 and EURP11 and QETH11. Moreover, evidence was found that HASH11 can act as a weak hedge against the Brazilian market.

For the C-vine, the independence observed between the asset pair EURP11 and QBTC11, when conditioned on information from HASH11, represents a potential diversification opportunity. The low association between EURP11 and QETH11 under the same conditions suggests that Ethereum could serve as a weak hedge against the European market. Another diversification opportunity would be to invest in SHY and QBTC11 when the investor is aware of the signals emitted from EURP11 and HASH11.

In the D-vine estimation, a hedging potential was identified by investing in HASH11 against IVVB11 when conditioned on QETH11. Allocating to Bitcoin and the Chinese market may offer a diversification opportunity when conditioned on HASH11, QETH11, IVVB11, and EURP11. The S&P 500 proved to be a safe haven relative to the Brazilian market when this relationship is conditioned on the crypto-asset ETFs.

In light of the results obtained, we can adopt strategies that best match the risk profiles of different investors. This study is pioneering in examining how this new class of ETFs relates to other conventional funds. As an extension of this work, it is suggested to analyze how these copula models perform when incorporated into portfolio-optimization frameworks and to conduct that analysis using time-varying vine copulas; moreover, other crypto-related ETFs that were left out could be included in the study, or an analysis could be carried out focusing exclusively on this group.

References

- Aas, K., Czado, C., Frigessi, A. and Bakken, H. (2009). Pair-copula constructions of multiple dependence, *Insurance: Mathematics and economics*, 44(2), 182–198.
- Almeida, J. and Gonçalves, T. C. (2022). Portfolio diversification, hedge and safe-haven properties in cryptocurrency investments and financial economics: A systematic literature review, *Journal of Risk and Financial Management*, 16(1), 3.
- Bartoletti, M., Lande, S., Loddo, A., Pompianu, L. and Serusi, S. (2021). Cryptocurrency scams: analysis and perspectives, *Ieee Access*, 9, 148353–148373.

- Baur, D. G. and McDermott, T. K. (2010). Is gold a safe haven? international evidence, *Journal of Banking & Finance*, 34(8), 1886–1898.
- Baur, D. G. and McDermott, T. K. (2016). Why is gold a safe haven?, *Journal of Behavioral and Experimental Finance*, 10, 63–71.
- Bedford, T. and Cooke, R. M. (2002). Vines: a new graphical model for dependent random variables, *The Annals of Statistics*, 30(4), 1031–1068.
- Berg, D. and Aas, K. (2009). Models for construction of multivariate dependence: A comparison study, *The European Journal of Finance*, 15(7), 639–659.
- Boako, G., Tiwari, A. K. and Roubaud, D. (2019). Vine copula-based dependence and portfolio value-at-risk analysis of the cryptocurrency market, *International Economics*, 158, 77–90.
- Bollerslev, T. (1986). Generalized autoregressive conditional heteroskedasticity, *Journal of econometrics*, 31(3), 307–327.
- Bouri, E., Gil-Alana, L. A., Gupta, R. and Roubaud, D. (2019). Modelling long memory volatility in the bitcoin market: Evidence of persistence and structural breaks, *International Journal of Finance & Economics*, 24(1), 412–426.
- Brechmann, E. C., Czado, C. and Aas, K. (2012). Truncated regular vines in high dimensions with application to financial data, *Canadian journal of statistics*, 40(1), 68–85.
- Brechmann, E. C. and Joe, H. (2015). Truncation of vine copulas using fit indices, *Journal of Multivariate Analysis*, 138, 19–33.
- Burniske, C. and Tatar, J. (2017). *Cryptoassets: The innovative investor's guide to bitcoin and beyond*, McGraw Hill Professional.
- Buterin, V. et al. (2014). A next-generation smart contract and decentralized application platform, *white paper*, 3(37), 2–1.
- Charfeddine, L., Benlagha, N. and Khediri, K. B. (2022). An intracryptocurrency analysis of volatility connectedness and its determinants: Evidence from mining coins, non-mining coins and tokens, *Research in International Business and Finance*, 62, 101699.
- Charfeddine, L. and Benlagha, N. (2016). A time-varying copula approach for modelling dependency: New evidence from commodity and stock markets, *Journal of Multinational Financial Management*, 37, 168–189.
- Clarke, K. A. (2007). A simple distribution-free test for nonnested model selection, *Political Analysis*, 15(3), 347–363.
- Cooke, R. M., Joe, H. and Aas, K. (2010). Vines arise, *Dependence Modeling: Vine Copula Handbook*, World Scientific, Singapore, pp. 37–71.
- Czado, C. (2010). Pair-copula constructions of multivariate copulas, in P. Jaworski, F. Durante, W. K. Härdle and T. Rychlik (eds), *Copula Theory and*

- Its Applications*, number 198, Springer Berlin Heidelberg, Berlin, Heidelberg, pp. 93–109.
- Czado, C. (2019). Analyzing dependent data with vine copulas, *Lecture Notes in Statistics*, Springer, 222.
- Dißmann, J., Brechmann, E. C., Czado, C. and Kurowicka, D. (2013). Selecting and estimating regular vine copulae and application to financial returns, *Computational Statistics & Data Analysis*, 59, 52–69.
- Economica (2023). Raio-x dos fundos de Índices (etf) em 2022: Cotistas, volume e retornos.
- Gadi, M. F. A. and Sicilia, M.-A. (2022). Analyzing safe haven, hedging and diversifier characteristics of heterogeneous cryptocurrencies against g7 and brics market indexes, *Journal of Risk and Financial Management*, 15(12), 572.
- Gebka, B. and Wohar, M. E. (2013). Causality between trading volume and returns: Evidence from quantile regressions, *International Review of Economics & Finance*, 27, 144–159.
- Genest, C., Rémillard, B. and Beaudoin, D. (2009). Goodness-of-fit tests for copulas: A review and a power study, *Insurance: Mathematics and economics*, 44(2), 199–213.
- Goeking, W. (2021). Bolsa brasileira terá primeiro ETF de bitcoin da América Latina.
URL: <https://valorinveste.globo.com/mercados/cripto/noticia/2021/03/19/bolsa-brasileira-tera-primeiro-etf-de-bitcoin-da-america-latina.ghtml>
- Hu, L. (2006). Dependence patterns across financial markets: a mixed copula approach, *Applied financial economics*, 16(10), 717–729.
- Huang, J.-J., Lee, K.-J., Liang, H. and Lin, W.-F. (2009). Estimating value at risk of portfolio by conditional copula-garch method, *Insurance: Mathematics and economics*, 45(3), 315–324.
- Jeegers, T. (2023). *Understanding crypto fundamentals: Value investing in cryptoassets and management of underlying risks*, 1 ed., Apress, Berkley, California.
- Jeribi, A. and Fakhfekh, M. (2021). Portfolio management and dependence structure between cryptocurrencies and traditional assets: evidence from figarch-evt-copula, *Journal of Asset Management*, 22(3), 224–239.
- Joe, H. (1996). Families of m-variate distributions with given margins and m(m-1)/2 bivariate dependence parameters, *Lecture notes-monograph series*, pp. 120–141.
- Joe, H. and Kurowicka, D. (2011). *Dependence modeling: vine copula handbook*, World Scientific, Singapore.
- Joe, H. and Xu, J. J. (1996). The estimation method of inference functions for

- margins for multivariate models, , .
- Kolev, N., Anjos, U. d. and Mendes, B. V. d. M. (2006). Copulas: a review and recent developments, *Stochastic models*, 22(4), 617–660.
- Liu, Y. and Luger, R. (2009). Efficient estimation of copula-garch models, *Computational Statistics & Data Analysis*, 53(6), 2284–2297.
- Mai, J.-F. and Scherer, M. (2014). *Financial engineering with copulas explained*, Springer, Hampshire, UK.
- Makarov, I. and Schoar, A. (2020). Trading and arbitrage in cryptocurrency markets, *Journal of Financial Economics*, 135(2), 293–319.
- McNeil, A. J., Frey, R. and Embrechts, P. (2015). *Quantitative risk management: concepts, techniques and tools*, Princeton University Press, Princeton, New Jersey.
- Mensi, W., Hkiri, B., Al-Yahyaee, K. H. and Kang, S. H. (2018). Analyzing time–frequency co-movements across gold and oil prices with brics stock markets: A var based on wavelet approach, *International Review of Economics & Finance*, 54, 74–102.
- Mita, M., Ito, K., Ohsawa, S. and Tanaka, H. (2019). What is stablecoin?: A survey on price stabilization mechanisms for decentralized payment systems, *2019 8th International Congress on Advanced Applied Informatics (IIAI-AAI)*, IEEE, Toyama, Japan, pp. 60–66.
- Morales-Napoles, O. (2010). Counting vines, *Dependence modeling: Vine copula handbook*, World Scientific, Singapore, pp. 189–218.
- Nakamoto, S. (2008). Bitcoin: A peer-to-peer electronic cash system, , .
- Nelsen, R. B. (2006). *An introduction to copulas*, Springer, New York, New York.
- Nelson, D. B. (1991). Conditional heteroskedasticity in asset returns: A new approach, *Econometrica: Journal of the econometric society*, pp. 347–370.
- Osman, M. B., Galariotis, E., Guesmi, K., Hamdi, H. and Naoui, K. (2023). Diversification in financial and crypto markets, *International Review of Financial Analysis*, 89, 102785.
- Poon, S.-H., Rockinger, M. and Tawn, J. (2004). Extreme value dependence in financial markets: Diagnostics, models, and financial implications, *The Review of Financial Studies*, 17(2), 581–610.
- Shih, J. H. and Louis, T. A. (1995). Inferences on the association parameter in copula models for bivariate survival data, *Biometrics*, pp. 1384–1399.
- Sklar, M. (1959). Fonctions de répartition à n dimensions et leurs marges, *Annales de l'ISUP*, Vol. 8, Publications de l'Institut de Statistique de l'Université de Paris, Paris, pp. 229–231.
- Statista (2023). Number of cryptocurrencies worldwide from 2013 to january 2024, *Statista*, .

- Suratkar, S., Shirole, M. and Bhirud, S. (2020). Cryptocurrency wallet: A review, *2020 4th international conference on computer, communication and signal processing (ICCCSP)*, IEEE, Chennai, pp. 1–7.
- Talbi, M., Bedoui, R., De Peretti, C. and Belkacem, L. (2021). Is the role of precious metals as precious as they are? a vine copula and bivar approaches, *Resources Policy*, 73, 102140.
- Vuong, Q. H. (1989). Likelihood ratio tests for model selection and non-nested hypotheses, *Econometrica: journal of the Econometric Society*, pp. 307–333.
- Xia, P., Wang, H., Zhang, B., Ji, R., Gao, B., Wu, L., Luo, X. and Xu, G. (2020). Characterizing cryptocurrency exchange scams, *Computers & Security*, 98, 101993.
- Yahoo Finance (2024). Historical stock price data for multiple companies. Dataset accessed via API using R.
URL: <https://finance.yahoo.com/>
- Yi, S., Xu, Z. and Wang, G.-J. (2018). Volatility connectedness in the cryptocurrency market: Is bitcoin a dominant cryptocurrency?, *International Review of Financial Analysis*, 60, 98–114.
- Zhang, W., Wang, P., Li, X. and Shen, D. (2018). Some stylized facts of the cryptocurrency market, *Applied Economics*, 50(55), 5950–5965.

A. Tables

Table 9
Estimated R-Vine model

Tree	Edge	Copula	Parameter 1	Parameter 2	τ	λ_u	λ_l	
1	1,2	t	0.87	4.27	0.67	0.56	0.56	
	1,3	t	0.85	5.13	0.64	0.50	0.50	
	5,1	F	2.78	-	0.29	-	-	
	10,9	t	0.68	5.58	0.47	0.30	0.30	
	4,6	G270	-1.31	-	-0.24	-	-	
	4,10	G	1.19	-	0.16	0.21	-	
	7,4	G	1.29	-	0.23	0.29	-	
	7,5	t	0.77	8.00	0.56	0.31	0.31	
	8,7	t	0.51	5.97	0.34	0.18	0.18	
	2	3,2:1	SG	1.13	-	0.12	-	0.16
		5,3:1	G	1.06	-	0.05	0.07	-
		7,1:5	F	0.81	-	0.09	-	-
		4,9:10	I	-	-	0.00	-	-
		10,6:4	SG	1.08	-	0.07	-	0.10
7,10:4		I	-	-	0.00	-	-	
8,4:7		C	0.13	-	0.06	-	0.00	
8,5:7		I	-	-	0.00	-	-	
3	5,2:3,1	I	-	-	0.00	-	-	
	7,3:5,1	I	-	-	0.00	-	-	
	8,1:7,5	I	-	-	0.00	-	-	
	6,9:4,10	I	-	-	0.00	-	-	
	7,6:10,4	SJ	1.08	-	0.04	-	0.10	
	8,10:7,4	I	-	-	0.00	-	-	
	5,4:8,7	I	-	-	0.00	-	-	
	7,2:5,3,1	I	-	-	0.00	-	-	
4	8,3:7,5,1	I	-	-	0.00	-	-	
	4,1:8,7,5	I	-	-	0.00	-	-	
	7,9:6,4,10	I	-	-	0.00	-	-	
	8,6:7,10,4	F	0.79	-	0.09	-	-	
	5,10:8,7,4	I	-	-	0.00	-	-	
	8,2:7,5,3,1	I	-	-	0.00	-	-	
	4,3:8,7,5,1	I	-	-	0.00	-	-	
	10,1:4,8,7,5	I	-	-	0.00	-	-	
5	8,9:7,6,4,10	G270	-1.06	-	-0.06	-	-	
	5,6:8,7,10,4	I	-	-	0.00	-	-	
	4,2:8,7,5,3,1	I	-	-	0.00	-	-	
	10,3:4,8,7,5,1	I	-	-	0.00	-	-	
	6,1:10,4,8,7,5	C	0.18	-	0.08	-	0.02	
6	5,9:8,7,6,4,10	I	-	-	0.00	-	-	
	10,2:4,8,7,5,3,1	I	-	-	0.00	-	-	
	6,3:10,4,8,7,5,1	I	-	-	0.00	-	-	
7	9,1:6,10,4,8,7,5	I	-	-	0.00	-	-	
	6,2:10,4,8,7,5,3,1	I	-	-	0.00	-	-	
8	9,3:6,10,4,8,7,5,1	I	-	-	0.00	-	-	
	9,2:6,10,4,8,7,5,3,1	I	-	-	0.00	-	-	
9	9,2:6,10,4,8,7,5,3,1	I	-	-	0.00	-	-	
BIC = -2497.23								
GoF: KS = 0.1717917 p-value = 1 CvM = 0.002654056 p-value = 1								

Note: The numbers 1, 2, 3, 4, 5, 6, 7, 8, 9 e 10 are respectively the ETFs: HASH11, QBTC11, QETH11, GOLD11, IVVB11, BOVA11, EURP11, XINA11, TIP and SHY.

Table 10
Estimated C-Vine model

Tree	Edge	Copula	Parameter 1	Parameter 2	τ	λ_u	λ_l
1	1,2	t	0.87	4.27	0.67	0.56	0.56
	1,4	J	1.10	-	0.06	0.13	-
	1,5	F	2.78	-	0.29	-	-
	1,8	F	1.67	-	0.18	-	-
	1,3	t	0.85	5.13	0.64	0.50	0.50
	1,6	C	0.21	-	0.10	-	0.04
	1,9	I	-	-	0.00	-	-
	1,7	F	2.63	-	0.27	-	-
	10,1	J	1.09	-	0.05	0.11	-
	-	-	-	-	0.00	-	-
2	7,2:1	I	-	-	0.00	-	-
	7,4:1	F	2.38	-	0.25	-	-
	7,5:1	t	0.73	8.00	0.52	0.27	0.27
	7,8:1	t	0.45	6.12	0.30	0.14	0.14
	7,3:1	G	1.06	-	0.06	0.08	-
	7,6:1	G270	-1.09	-	-0.08	-	-
	7,9:1	J	1.08	-	0.04	0.10	-
10,7:1	I	-	-	0.00	-	-	
3	10,2:7,1	I	-	-	0.00	-	-
	10,4:7,1	G	1.18	-	0.15	0.20	-
	10,5:7,1	I	-	-	0.00	-	-
	10,8:7,1	I	-	-	0.00	-	-
	10,3:7,1	I	-	-	0.00	-	-
	10,6:7,1	I	-	-	0.00	-	-
	10,9:7,1	t	0.68	7.14	0.47	0.25	0.25
4	6,2:10,7,1	I	-	-	0.00	-	-
	6,4:10,7,1	N	-0.38	-	-0.25	-	-
	6,5:10,7,1	I	-	-	0.00	-	-
	6,8:10,7,1	I	-	-	0.00	-	-
	6,3:10,7,1	I	-	-	0.00	-	-
	9,6:10,7,1	I	-	-	0.00	-	-
5	3,2:6,10,7,1	SG	1.14	-	0.12	-	0.16
	3,4:6,10,7,1	I	-	-	0.00	-	-
	3,5:6,10,7,1	I	-	-	0.00	-	-
	3,8:6,10,7,1	I	-	-	0.00	-	-
	9,3:6,10,7,1	I	-	-	0.00	-	-
6	8,2:3,6,10,7,1	I	-	-	0.00	-	-
	8,4:3,6,10,7,1	C	0.18	-	0.08	-	0.02
	8,5:3,6,10,7,1	I	-	-	0.00	-	-
	9,8:3,6,10,7,1	I	-	-	0.00	-	-
7	5,2:8,3,6,10,7,1	I	-	-	0.00	-	-
	5,4:8,3,6,10,7,1	J	1.10	-	0.05	0.12	-
	9,5:8,3,6,10,7,1	I	-	-	0.00	-	-
8	9,2:5,8,3,6,10,7,1	I	-	-	0.00	-	-
	9,4:5,8,3,6,10,7,1	I	-	-	0.00	-	-
9	4,2:9,5,8,3,6,10,7,1	I	-	-	0.00	-	-

BIC = -2499,44

GoF: KS = 0.2864268 | p-valor = 0.74 | CvM = 0.003085683 | p-valor = 1

Note: The numbers 1, 2, 3, 4, 5, 6, 7, 8, 9 e 10 are respectively the ETFs: HASH11, QBTC11, QETH11, GOLD11, IVVB11, BOVA11, EURP11, XINA11, TIP and SHY.

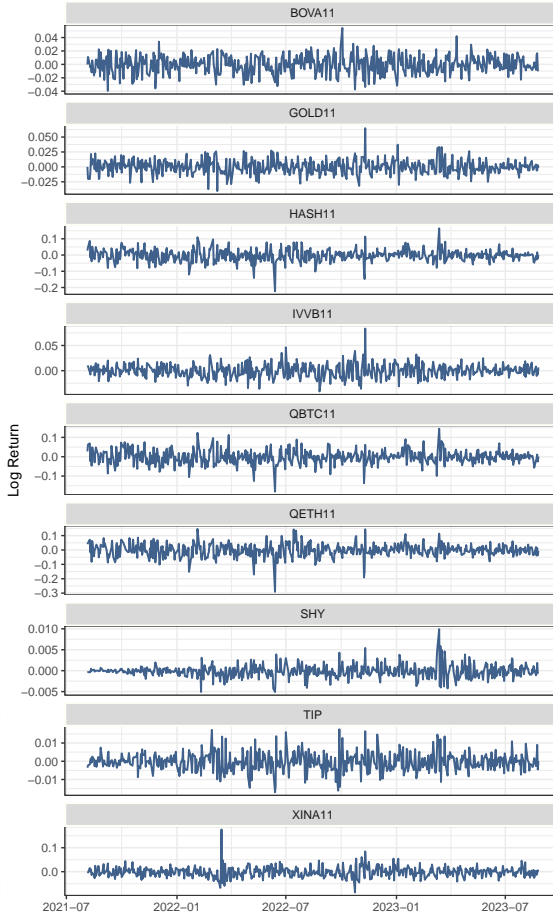
Table 11
Estimated D-Vine model

Tree	Edge	Copula	Parameter 1	Parameter 2	τ	λ_u	λ_l			
1	7,8	t	0.51	5.97	0.34	0.18	0.18			
	5,7	t	0.77	8.00	0.56	0.31	0.31			
	3,5	F	2.57	-	0.27	-	-			
	1,3	t	0.85	5.13	0.64	0.50	0.50			
	2,1	t	0.87	4.27	0.67	0.56	0.56			
	6,2	SJ	1.19	-	0.10	-	0.21			
	4,6	G270	-1.31	-	-0.24	-	-			
	9,4	G	1.14	-	0.12	0.16	-			
	10,9	t	0.68	5.58	0.47	0.30	0.30			
	2	5,8;7	I	-	-	0.00	-	-		
3,7;5		I	-	-	0.00	-	-			
1,5;3		SG	1.11	-	0.10	-	0.14			
2,3;1		SG	1.13	-	0.12	-	0.16			
6,1;2		I	-	-	0.00	-	-			
4,2;6		G	1.07	-	0.07	0.09	-			
9,6;4		SG	1.09	-	0.08	-	0.11			
10,4;9		G	1.12	-	0.11	0.14	-			
3		3,8;5,7	I	-	-	0.00	-	-		
		1,7;3,5	I	-	-	0.00	-	-		
	2,5;1,3	I	-	-	0.00	-	-			
	6,3;2,1	I	-	-	0.00	-	-			
	4,1;6,2	I	-	-	0.00	-	-			
	9,2;4,6	I	-	-	0.00	-	-			
	10,6;9,4	I	-	-	0.00	-	-			
	4	1,8;3,5,7	I	-	-	0.00	-	-		
		2,7;1,3,5	I	-	-	0.00	-	-		
		6,5;2,1,3	G90	-1.11	-	-0.10	-	-		
4,3;6,2,1		I	-	-	0.00	-	-			
9,1;4,6,2		I	-	-	0.00	-	-			
10,2;9,4,6		I	-	-	0.00	-	-			
5		2,8;1,3,5,7	I	-	-	0.00	-	-		
		6,7;2,1,3,5	I	-	-	0.00	-	-		
		4,5;6,2,1,3	F	1.64	-	0.18	-	-		
		9,3;4,6,2,1	I	-	-	0.00	-	-		
	10,1;9,4,6,2,1	I	-	-	0.00	-	-			
	6	6,8;2,1,3,5,7	I	-	-	0.00	-	-		
		4,7;6,2,1,3,5	G	1.17	-	0.14	0.19	-		
		9,5;4,6,2,1,3	I	-	-	0.00	-	-		
		10,3;9,4,6,2,1	I	-	-	0.00	-	-		
		7	4,8;6,2,1,3,5,7	C	0.16	-	0.07	-	0.01	
9,7;4,6,2,1,3,5			I	-	-	0.00	-	-		
10,5;9,4,6,2,1			I	-	-	0.00	-	-		
8			9,8;4,6,2,1,3,5,7	G90	-1.08	-	-0.07	-	-	
			10,7;9,4,6,2,1,3,5	I	-	-	0.00	-	-	
			9	10,8;9,4,6,2,1,3,5,7	I	-	-	0.00	-	-
	BIC = -2503.13									
	GoF: KS = 0.2447613 p-valor = 0.945 CvM = 0.00235645 p-valor = 1									

Note: The numbers 1, 2, 3, 4, 5, 6, 7, 8, 9 e 10 are respectively the ETFs: HASH11, QBTC11, QETH11, GOLD11, IVVB11, BOVA11, EURP11, XINA11, TIP and SHY.

B. Figures

Figure 2
Daily log returns of the selected ETFs



Source: [Yahoo Finance](#) (2024).